

Exclusive C–C Oxidative Addition in a Rhodium Thiophosphoryl Pincer Complex and Computational Evidence for an η^3 -C–C–H Agostic Intermediate

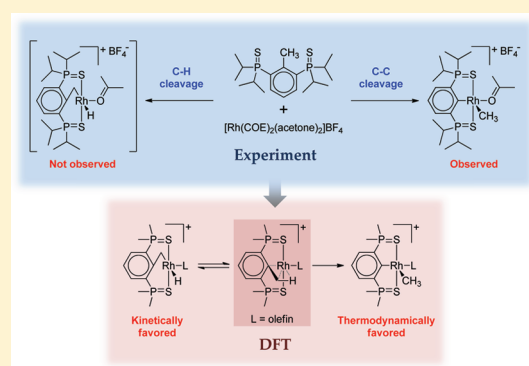
Michael Montag,^{†,||} Irena Efremenko,^{†,||} Yael Diskin-Posner,[‡] Yehoshua Ben-David,[†] Jan M. L. Martin,^{†,§} and David Milstein^{*,†}

[†]Department of Organic Chemistry, Weizmann Institute of Science, Rehovot 76000, Israel

[‡]Department of Chemical Research Support, Weizmann Institute of Science, Rehovot 76000, Israel

Supporting Information

ABSTRACT: The room-temperature reaction between the Rh(I) precursor $[\text{Rh}(\text{COE})_2(\text{acetone})_2]\text{BF}_4$ (COE = cyclooctene) and a new thiophosphoryl-based SCS pincer ligand leads to oxidative addition of an sp^2 – sp^3 C–C bond as the only observed outcome, despite the presence of accessible sp^3 C–H bonds. A DFT study reveals that the chemistry of the SCS system is controlled by π repulsion between occupied rhodium d orbitals and the lone-pair electrons on the two sulfur atoms. This repulsion gives rise to the thermodynamic selectivity for C–C over C–H cleavage, as it is attributed to the higher electronegativity of a methyl versus hydride ligand, thereby allowing more effective release of excessive π electron density. It is also demonstrated that the observed C–C and unobserved C–H cleavage pathways originate from a common intermediate that features a novel η^3 -C–C–H agostic interaction. The COE ligand is shown to play an important role by greatly stabilizing this intermediate, making it the only available entry point to both reaction pathways.

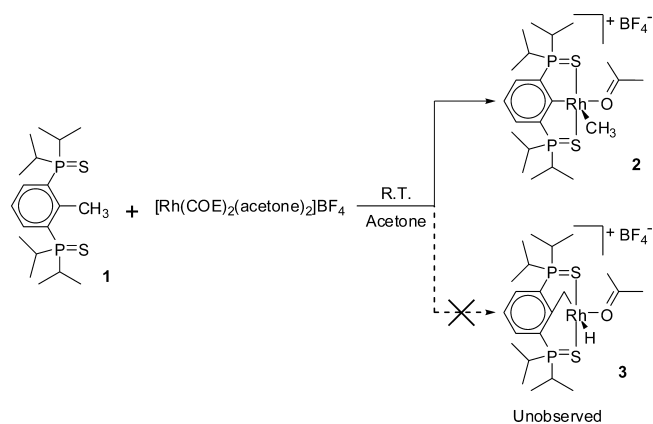


INTRODUCTION

Selective activation of nonstrained carbon–carbon single bonds by transition metals is one of the fundamental challenges of modern organometallic chemistry.^{1,2} Mechanistic insights regarding such reactions have been obtained with pincer ligands,^{3,4} which provide a highly controlled steric and electronic environment for metal centers. These studies have primarily involved phosphorus-based pincer ligands, wherein one ligand arm bears a strongly coordinating phosphorus donor group (typically phosphine), and the second arm bears a donor group of varying lability, such as phosphine (PCP), amine (PCN), or ether (PCO).³ Much less attention has been devoted to other pincer systems,⁵ even though a diverse range of pincer ligands is available. One type of ligands that has not been explored vis-à-vis C–C activation is the thiophosphoryl-based pincers.⁶ These ligands feature soft sulfur donors that are suitable for binding late transition metals and are typically air-stable, in contrast to the commonly employed phosphorus donor ligands.

Herein, we describe the reaction of the new thiophosphoryl SCS-type pincer ligand **1** (Scheme 1) with the cationic Rh(I) precursor $[\text{Rh}(\text{COE})_2(\text{acetone})_2]\text{BF}_4$ (COE = cyclooctene), which resulted in exclusive oxidative addition of a strong sp^2 – sp^3 C–C bond. The observed preference of the SCS system toward cleavage of this bond, rather than the more numerous and accessible sp^3 C–H bonds of the Ar–CH₃ moiety, was

Scheme 1. Exclusive C–C Oxidative Addition upon Reaction of the Thiophosphoryl SCS Ligand with a Rh(I) Precursor



probed computationally. This revealed the root cause of the selectivity to be significant Rh–S π repulsion, and the fact that this repulsion can be better reduced by the methyl ligand of the C–C cleavage product than by the less electronegative hydride ligand of the C–H cleavage product. The resulting thermody-

Received: December 2, 2011

Published: December 28, 2011

namic selectivity for C–C cleavage is further enhanced by high reversibility of the kinetically favored C–H cleavage reaction. Intriguingly, the reaction pathways for C–C and C–H cleavage were found to share a common intermediate featuring a hitherto unreported η^3 -C–C–H agostic interaction.

RESULTS AND DISCUSSION

As shown in Scheme 1, when an acetone solution of $[\text{Rh}(\text{COE})_2(\text{acetone})_2]\text{BF}_4$ was treated with 1 equiv of ligand **1**⁷ at room temperature, a facile C–C cleavage reaction ensued, resulting in the gradual formation of complex **2** over several hours.⁸ The reaction product was isolated in high yield (~90%) and characterized by solution NMR techniques, as well as single-crystal X-ray crystallography. The $^{31}\text{P}\{^1\text{H}\}$ NMR spectrum of **2** in acetone- d_6 exhibits a sharp singlet at 80.63 ppm, and its ^1H NMR spectrum features a broad singlet at 1.37 ppm, which was assigned to the methyl ligand. The latter also gives rise to a doublet at -6.77 ppm ($^1J_{\text{RhC}} = 26.2$ Hz) in the $^{13}\text{C}\{^1\text{H}\}$ NMR spectrum. Both the ^1H and the $^{13}\text{C}\{^1\text{H}\}$ NMR spectra of **2** are consistent with a meridionally coordinated pincer ligand and an axial methyl ligand (overall C_s molecular symmetry), as corroborated by crystallographic analysis (see below). The $^{19}\text{F}\{^1\text{H}\}$ NMR spectrum features a sharp singlet at -152.51 ppm, indicative of a noncoordinated BF_4^- counterion.

An attempt to crystallize complex **2** from acetone yielded crystals of its adduct with diacetone alcohol (4-hydroxy-4-methyl-2-pentanone), complex **2a**. The solid-state structure of this complex (Figure 1) exhibits a rhodium atom situated in an

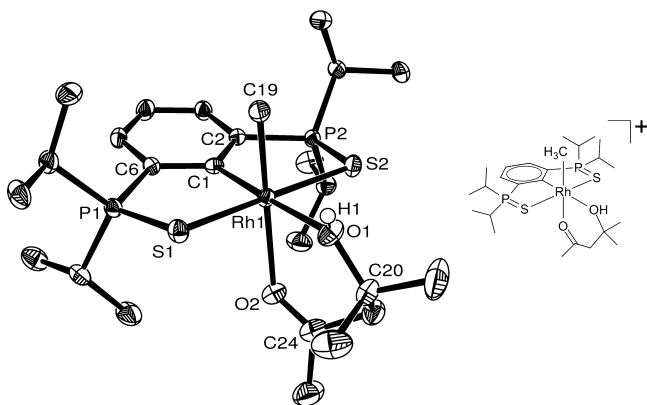


Figure 1. ORTEP drawing (50% probability level) of complex **2a**, the adduct of complex **2** with diacetone alcohol (4-hydroxy-4-methyl-2-pentanone). All hydrogen atoms (except H1) and BF_4^- were omitted for clarity. Selected bond distances (Å) and angles (deg) for complex **2**: Rh1–C1, 1.971(2); Rh1–C19, 2.031(2); Rh1–O1, 2.2336(18); Rh1–O2, 2.2612(18); Rh1–S1, 2.3579(6); Rh1–S2, 2.3730(6); C1–Rh1–C19, 85.88(9); C1–Rh1–S1, 91.86(6); C1–Rh1–S2, 92.03(6); C1–Rh1–O1, 177.49(8); C1–Rh1–O2, 99.45(8).

octahedral environment that is defined by a meridionally coordinated SCS ligand, an axial methyl moiety, and the chelating ketol. The BF_4^- counterion is outer-sphere (not shown in Figure 1), in agreement with the solution ^{19}F NMR spectrum, but does interact with the complex via H-bonding to the OH group of the ketol. The ketol ligand was not detected by solution NMR techniques, nor implicated by elemental analysis of a bulk sample of the complex. It might have been produced in situ by rhodium-promoted aldol condensation of two acetone molecules.⁹

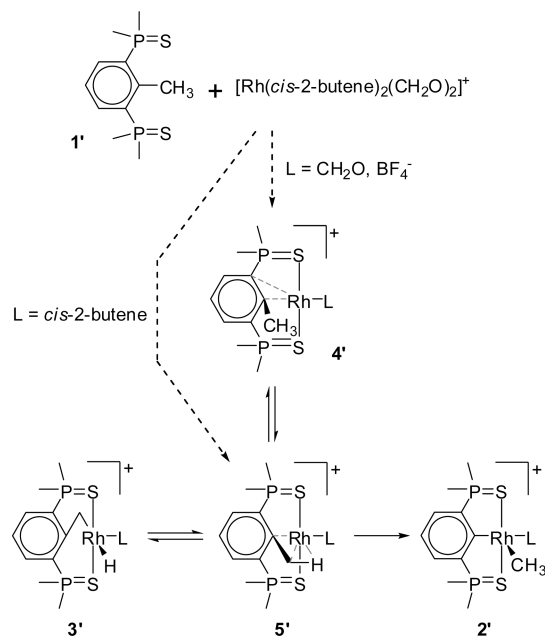
Complex **2** was the only observed reaction product in acetone, and its gradual formation over several hours was not accompanied by C–H cleavage products. Of particular significance was the absence of sp^3 C–H cleavage product **3** (Scheme 1), the analogues of which had been observed in previous pincer systems.^{4c,d,h,i,j,k,n,q} Moreover, no C–H cleavage products were detected when the solution containing **2** was heated at 60 °C for 12 h. We have previously shown that phosphine-based pincer ligands that are structurally analogous to **1** may undergo concurrent or consecutive sp^3 C–H and sp^2 – sp^3 C–C bond activations upon reaction with various transition-metal precursors.^{4c,d,h,i,j,k,n,q} In one notable case, the reaction could be directed toward either C–C or C–H oxidative addition simply by changing the solvent.⁴ⁱ In that instance, when the reaction was carried out in THF, exclusive C–C cleavage was observed, whereas in the presence of acetonitrile only C–H cleavage occurred. In light of these results, we repeated the reaction of ligand **1** with the Rh(I) precursor in solvents of varying donicity, that is, THF (THF- d_8 /CD $_2$ Cl $_2$, 1:1),¹⁰ methanol (CD $_3$ OD/CD $_2$ Cl $_2$, 1:1),¹¹ and acetonitrile (18 equiv of CD $_3$ CN in acetone- d_6).¹² Nevertheless, only C–C cleavage was observed in all cases, supporting the conclusion that the thiophosphoryl SCS system is exclusively selective toward C–C bond cleavage.

Exclusive C–C cleavage has been previously observed in rhodium complexes of PCN¹³ and POCOP¹⁴ (phosphinite-based) pincer ligands. The differences in selectivity between these systems and earlier PCP complexes, which exhibited both C–C and C–H activation, were attributed to differences in ligand arm length. It was suggested that the amine and phosphinite arms draw the metal ion closer to the C–C bond than do the longer phosphine arms of the PCP ligands, thereby favoring C–C over C–H activation. Nevertheless, the present results are not in line with this explanation, since the thiophosphoryl arms of the SCS ligand are longer than those of previously reported PCP ligands,¹⁵ and yet the SCS system exhibits exclusive C–C cleavage.

To probe the energetic and electronic basis for the observed selectivity of the SCS system, we undertook a density functional theory (DFT) study of the mechanisms of both sp^2 – sp^3 C–C and sp^3 C–H oxidative addition, using model structures as shown in Scheme 2. The mechanisms were examined in the absence of ancillary ligands, as well as in the presence of the experimentally relevant, electron-donating ligands CH $_2$ O (acetone model) and BF_4^- , and the electron-withdrawing ligand *cis*-2-butene (cyclooctene model). The computed reaction profiles for C–C and C–H cleavage are displayed in Figure 2. The C–C cleavage product, **2'**, is thermodynamically stable for all of the examined ancillary ligands, and even in their absence. By contrast, formation of the C–H cleavage product, **3'**, is considerably less favorable than **2'** and is even endergonic in the absence of an ancillary ligand or with CH $_2$ O. This clearly indicates that C–C oxidative addition is thermodynamically preferred for the SCS system, in agreement with the experimental results, as well as previous computational investigations of C–C versus C–H cleavage in pincer systems.^{4n,16}

In addition to the reaction products, two precleaved intermediates were also located as minima on the potential energy surface (PES). The first structure, complex **4'**, exhibits no bonding interactions between the metal and the adjacent methyl moiety, but features η^2 arene–metal coordination, as previously found for an analogous PCN–Rh(I) pincer

Scheme 2. Model Structures Used for the DFT Examination of Oxidative Addition of sp^2 – sp^3 C–C and sp^3 C–H Bonds in the SCS System



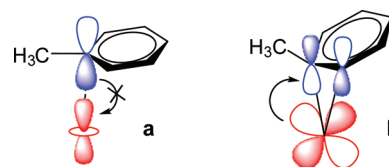
system.^{16c} In the latter case, preference for the η^2 structure was attributed to the short length of the amine arm, such that the metal center is constrained near the arene ring and prevented from effectively interacting with the methyl moiety. However, this geometrical argument does not apply in the SCS case, as this pincer ligand exhibits much longer arms.

The second reaction intermediate, complex 5', is located along the reaction pathways connecting 4' with products 2' and 3'.¹⁷ Interestingly, this intermediate features a novel η^3 -C–C–H agostic interaction, wherein the metal center interacts simultaneously with the sp^2 – sp^3 C–C and sp^3 C–H bonds. To the best of our knowledge, such an intermediate has not been previously found for the oxidative addition of either C–C or C–H bonds. Instead, earlier DFT investigations of pincer

systems have found η^1 -arene, η^2 -arene, and sp^3 C–H agostic species.^{4n,16} Generally speaking, the vast majority of agostic interactions reported to date involve η^2 -bound C–H bonds,¹⁸ whereas C–C agostic interactions have seldom been observed.^{4p,19} It is important to emphasize that the η^3 -C–C–H agostic interaction in 5' differs markedly from the well-documented β -agostic interaction,²⁰ despite their structural resemblance. In the former, all three atoms are anchored to the metal center through noncovalent dative bonding, whereas in the latter the alkyl group features a fully fledged M–C covalent bond. The fact that the η^3 -C–C–H agostic interaction has not been previously reported should be attributed not only to the unique characteristics of the SCS system but also to the relatively large polarization consistent basis set applied in the present calculations. It has been previously demonstrated that polarization functions have conceptual importance in representing weak electron back-donation effects.²¹ The relevance of η^3 -C–C–H agostic interactions to other pincer systems will be addressed in a future report.

Electronic structure analysis reveals that strong π repulsion between occupied S p and Rh d orbitals is a key factor that determines the stability and reactivity of the SCS–Rh complexes. Thus, charge decomposition analysis (CDA) indicates that arene \rightarrow Rh electron donation, which is the dominant component of the η^1 -arene interaction (Scheme 3a),

Scheme 3. Key Electronic Interaction in an η^1 -Arene Structure (a) and Its Stabilization by Electron Transfer to the Arene Ring, Leading to an η^2 -Arene Structure (b) as in Intermediate 4'



is energetically unfavorable in the electron-rich SCS system. Consequently, the system adopts the η^2 -arene configuration (Scheme 3b) that characterizes 4' and enables partial release of

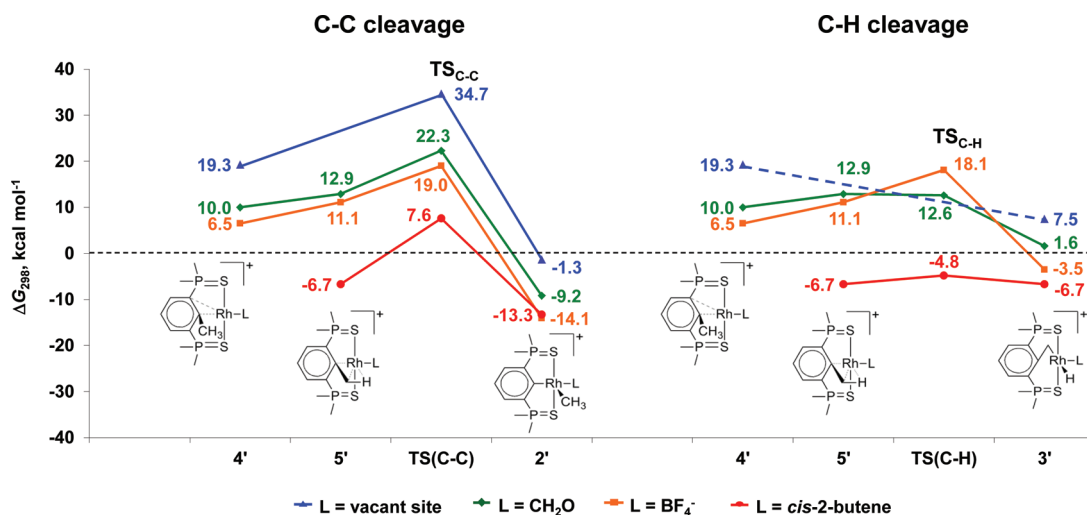
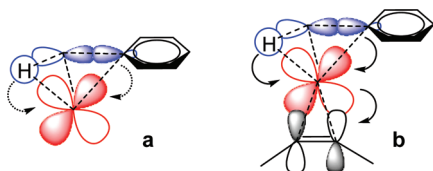


Figure 2. Computed reaction profiles for the oxidative addition of sp^2 – sp^3 C–C and sp^3 C–H bonds in the SCS system as a function of ancillary ligand (L). For L = vacant site, 5' and TS_{C-H} could not be located on the potential energy surface (PES). For L = *cis*-2-butene, 4' could not be located on the PES. Energies are referenced to the reactants, $[Rh(cis\text{-}2\text{-butene})_2(CH_2O)_2]^+ + 1'$.

excessive π electron density via Rh \rightarrow arene back-donation into high-lying empty arene π^* orbitals. Agostic complex $5'$ is characterized by a further increase in the C–C–H \rightarrow Rh electron donation (Scheme 4a). The overall interaction

Scheme 4. Key Electronic Interaction in the η^3 -C–C–H Agostic Intermediate $5'$ (a) and Its Stabilization by *cis*-2-Butene through Metal-to-Olefin Electron Transfer (b)



between the Ar–CH₃ fragment of $5'$ and the remainder of this complex, as found by CDA, is 5.9 kcal mol^{−1} stronger than in η^2 -arene complex $4'$.²² However, increased Rh–S π repulsion ultimately renders complex $5'$ a few kcal mol^{−1} less stable than $4'$, and both intermediates are thermodynamically unstable with respect to the reactants, as well as the C–C and C–H cleavage products. It should be noted that, in the absence of ancillary ligands, complex $5'$ could not be located on the PES, whereas $4'$ constitutes a direct precursor for both $2'$ and $3'$. In the presence of ancillary ligands, $5'$ becomes the immediate precursor for $2'$ and $3'$, thereby constituting a direct entry point to both C–C and C–H cleavage.

Dramatic changes in the electronic and energetic properties of the SCS system take place when the electron-withdrawing olefin, *cis*-2-butene, is introduced as an ancillary ligand, modeling the experimentally employed cyclooctene. In this case, the Rh \rightarrow arene electron donation becomes less important, and consequently complex $4'$ could not be located on the PES. By contrast, the η^3 -C–C–H agostic interaction is strongly reinforced by Rh \rightarrow olefin π back-bonding, which facilitates electron donation from the occupied σ_{C-C} and σ_{C-H} orbitals of the Ar–CH₃ moiety to the metal (Scheme 4b). This stabilizes complex $5'$ to an extraordinary extent, making it thermodynamically stable and isergonic with the C–H cleavage product $3'$. Thus, the olefin adduct of $5'$ is the most prevalent reaction intermediate within the SCS system, and is *the only feasible gateway to C–C and C–H cleavage in this system*.

The transition state for C–H cleavage (TS_{C-H}) is lower in energy than the corresponding one for C–C cleavage (TS_{C-C}), regardless of the ancillary ligand, thereby making C–H oxidative addition kinetically favored. This is in agreement with both experimental and computational results for previously reported pincer systems.^{4c,h,i,k,n,q,16} From the electronic structure perspective, the transition states of both C–C and C–H cleavage are characterized by further strengthening of the interaction between the metal center and the Ar–CH₃ fragment (by 13.3 and 11.9 kcal mol^{−1}, respectively), because of an increase in both electron donation and back-donation. Nevertheless, despite the high electron density on rhodium, it is a poor electron donor, because of the low energy of its occupied orbitals. Consequently, the buildup of electron charge at the metal center increases the Rh–S π repulsion. Because the C–C \rightarrow Rh donation is larger than C–H \rightarrow Rh (0.15 vs 0.06 electrons, respectively), the resulting Rh–S repulsion is stronger in the former case, thus leading to a late transition state and higher activation barrier for C–C cleavage. Conversely, C–H cleavage occurs through an early

transition state and its energy barrier is lower. It should nevertheless be noted that once $5'$ is formed the intrinsic kinetic barriers to both C–C and C–H cleavage are highly accessible at room temperature ($\Delta G_{298}^\ddagger \leq 14.3$ kcal mol^{−1}), such that both reactions are very facile.

It is important to stress that the behavior of the SCS system is dominated by its olefin adduct. This was shown above to be the only attainable entry point to C–C and C–H cleavage, and it is therefore the olefin adduct that determines the selectivity of the system. In this case, the extremely low barrier for C–H cleavage, and the fact that $3'$ and $5'$ are essentially isergonic, renders C–H oxidative addition highly reversible. Therefore, complex $2'$ is obtained as the only reaction product, in agreement with the experimental findings.²³ It is important to emphasize that the above kinetic considerations pertain only to the selectivity of the SCS system, whereas the apparent rate of C–C cleavage is probably determined by processes that precede the formation of complexes $4'$ and $5'$; for example, solvent or olefin detachment from the Rh(I) precursor.

Finally, electron transfer from rhodium to the sp²–sp³ C–C or sp³ C–H bond ultimately leads to their dissociation, thereby affording complexes $2'$ and $3'$, respectively. Hence, it is this charge transfer that determines the thermodynamic balance of the overall processes. CDA shows that preference for the C–C cleavage product arises from the significantly higher electro-negativity of the methyl ligand in $2'$ relative to the hydride in $3'$, which renders the Rh \rightarrow C–C electron transfer more effective than Rh \rightarrow C–H (with total donations of 0.49 and 0.37 electrons, respectively). Consequently, bonding in the Ar–Rh–CH₃ fragment is 12.5 kcal mol^{−1} stronger than in the ArCH₂–Rh–H fragment.

CONCLUSION

In summary, we have shown that the new thiophosphoryl-based SCS pincer ligand **1** reacts with the Rh(I) precursor [Rh(COE)₂(acetone)₂]₂BF₄ to undergo sp²–sp³ C–C bond cleavage as the only observed outcome, even though sp³ C–H bonds are also available for activation. A DFT study demonstrated that the chemistry of the SCS system is controlled by significant repulsion between occupied rhodium d orbitals and the lone-pair electrons on the two sulfur atoms. The selectivity for C–C cleavage was shown to be thermodynamic, and this was linked to the higher electro-negativity of the resulting methyl ligand relative to the hydride ligand of the C–H cleavage product, thus allowing for more effective release of excessive π electron density. The selectivity is enhanced by the high reversibility of the kinetically favored C–H cleavage reaction. It was also shown that the C–C and C–H cleavage pathways originate from a common intermediate that features a novel η^3 -C–C–H agostic interaction. The COE ligand was found to play a significant role in the present SCS system, by greatly stabilizing the agostic intermediate and making it the only available entry point to both C–C and C–H cleavage.

EXPERIMENTAL SECTION

General Procedures. All experiments were carried out under an atmosphere of purified nitrogen in an MBraun MB 150B-G glovebox, or under purified argon in an MBraun Unilab glovebox. The complex [Rh(COE)₂(acetone)₂]₂BF₄ was prepared according to a literature procedure.²⁴ All solvents were reagent grade or better. All non-deuterated solvents were refluxed over sodium/benzophenone ketyl and distilled under argon. Deuterated solvents were used as received

and were degassed with argon and kept in the glovebox over 3 or 4 Å molecular sieves (except for acetone, which was dried with Drierite). Commercially available reagents were used as received. Crystal structures were drawn using the program ORTEP-3.²⁵

Analysis. NMR spectra (^1H , ^{13}C , ^{19}F , and ^{31}P) were recorded using Bruker Avance-400 and Bruker Avance-500 NMR spectrometers. All measurements were done at 20 °C, unless noted otherwise. ^1H and ^{13}C NMR chemical shifts are reported in parts per million relative to tetramethylsilane. ^1H NMR chemical shifts are referenced to the residual hydrogen signal of the deuterated solvent, and the ^{13}C NMR chemical shifts are referenced to the ^{13}C signal(s) of the deuterated solvent. ^{19}F NMR chemical shifts are reported in parts per million relative to CFCl_3 and referenced to an external solution of C_6F_6 in CDCl_3 . ^{31}P NMR chemical shifts are reported in parts per million relative to H_3PO_4 and referenced to an external 85% solution of phosphoric acid in D_2O . Abbreviations used in the description of NMR data are as follows: Ar, aryl; br, broad; s, singlet; d, doublet; t, triplet; q, quartet; m, multiplet. Electrospray (ES) mass spectrometry was performed at the Chemical Analysis Laboratory (Department of Chemical Research Support), Weizmann Institute of Science, using Micromass Platform LCZ 4000 (Micromass, Manchester, U.K.) with a cone voltage of 43 V, an extractor voltage of 4 V, and a desolvation temperature of 150 °C. Elemental analysis was performed at H. Kolbe Mikroanalytisches Laboratorium, Mülheim an der Ruhr, Germany.

Synthesis of Ligand 1. This new ligand was prepared in analogy to a literature procedure.⁷

Step 1: Synthesis of the Bisphosphine Precursor 2,6-Bis-(diisopropylphosphino)toluene. A 1 L Schlenk-type flask equipped with a magnetic stirring bar was loaded, in the nitrogen glovebox, with 5.00 g (20.0 mmol) of 2,6-dibromotoluene, 5.66 g (47.9 mmol) of diisopropylphosphine, 0.20 g (1.1 mmol) of PdCl_2 , 6.40 g (65.2 mmol) of KOAc, and 75 mL of DMF. The flask was then removed from the glovebox, and the mixture was stirred at 130 °C for 2 h, under argon, after which it was cooled to room temperature. A 400 mL portion of degassed water was then added. The resulting mixture was extracted with 2×400 mL of diethyl ether, under nitrogen, and the combined organic phases were dried with Na_2SO_4 . The mixture was then passed through a sintered-glass filter, and the resulting clear solution was reintroduced into the glovebox and placed under high vacuum to remove the solvent. The resulting solid residue was washed with cold pentane and again placed under vacuum to remove the solvent. This yielded 4.00 g (12.9 mmol, 61.6% yield) of the product as a cream-colored solid. $^{31}\text{P}\{^1\text{H}\}$ NMR (162 MHz, CDCl_3): -3.74 (s). ^1H NMR (400 MHz, CDCl_3): 7.32 (d, $^3J_{\text{HH}} = 7.6$ Hz, 2H, Ar-H), 7.12 (t, $^3J_{\text{HH}} = 7.5$ Hz, 1H, Ar-H), 2.85 (s, 3H, Ar- CH_3), 2.04 (m, $^3J_{\text{HH}} = 6.9$ Hz, 4H, $\text{PCH}(\text{CH}_3)_2$), 1.08 (dd, $^3J_{\text{PH}} = 14.8$ Hz, $^3J_{\text{HH}} = 7.0$ Hz, 12H, $\text{PCH}(\text{CH}_3)_2$), 0.86 (dd, $^3J_{\text{PH}} = 11.7$ Hz, $^3J_{\text{HH}} = 6.9$ Hz, 12H, $\text{PCH}(\text{CH}_3)_2$). $^{13}\text{C}\{^1\text{H}\}$ NMR (126 MHz, CDCl_3): 151.06 (t, $^2J_{\text{PC}} = 24.0$ Hz, Ar), 134.85 (d, $^1J_{\text{PC}} = 14.1$ Hz, $\text{C}_{\text{Ar-P}}$), 132.68 (s, Ar), 124.29 (s, Ar), 24.06 (m, $\text{PCH}(\text{CH}_3)_2$), 21.75 (t, $^2J_{\text{PC}} = 27.8$ Hz, $\text{C}_{\text{Ar-CH}_3}$), 20.17 (m, $\text{PCH}(\text{CH}_3)_2$), 19.15 (m, $\text{PCH}(\text{CH}_3)_2$). Assignment of the $^{13}\text{C}\{^1\text{H}\}$ NMR signals was confirmed by ^{13}C - ^1H heteronuclear correlation. Elemental analysis: Found: C, 70.24%; H, 10.52%. Calcd for $\text{C}_{19}\text{H}_{34}\text{P}_2$: C, 70.34%; H, 10.56%.

Step 2: Sulfurization of 2,6-Bis-(diisopropylphosphino)toluene. A solution of 327.0 mg (1.01 mmol) of 2,6-bis-(diisopropylphosphino)toluene in 3.2 mL of THF was added to a suspension of 64.5 mg (2.01 mmol) of elemental sulfur in 5.9 mL of THF, and the resulting clear solution was stirred at room temperature for 21 h. The solvent was then removed under vacuum overnight to yield 382.7 mg (0.98 mmol, 97.7% yield) of ligand 1 as a white solid. $^{31}\text{P}\{^1\text{H}\}$ NMR (162 MHz, acetone- d_6): 76.10 (s). ^1H NMR (400 MHz, acetone- d_6): 8.69 (m, $^3J_{\text{HH}} = 7.9$ Hz, 2H, Ar-H), 7.54 (m, $^3J_{\text{HH}} = 7.9$ Hz, 1H, Ar-H), 3.04 (s, 3H, Ar- CH_3), 2.91 (m, $^2J_{\text{PH}} = 13.6$ Hz, $^3J_{\text{HH}} = 6.8$ Hz, 4H, $\text{PCH}(\text{CH}_3)_2$), 1.31 (dd, $^3J_{\text{PH}} = 17.3$ Hz, $^3J_{\text{HH}} = 6.7$ Hz, 6H, $\text{PCH}(\text{CH}_3)_2$), 0.83 (dd, $^3J_{\text{PH}} = 17.9$ Hz, $^3J_{\text{HH}} = 7.0$ Hz, 6H, $\text{PCH}(\text{CH}_3)_2$). $^{13}\text{C}\{^1\text{H}\}$ NMR (101 MHz, acetone- d_6): 143.37 (bm, $\text{C}_{\text{Ar-Me}}$), 139.78 (d, $^2J_{\text{PC}} = 10.4$ Hz, Ar), 131.71 (dd, $^1J_{\text{PC}} = 61.8$ Hz, $^3J_{\text{PC}} = 8.0$ Hz, $\text{C}_{\text{Ar-P}}$), 125.84 (d, $^2J_{\text{PC}} = 11.8$ Hz, Ar), 29.53 (d, $^1J_{\text{PC}} = 49.9$ Hz, $\text{PCH}(\text{CH}_3)_2$), 22.41 (t, $^3J_{\text{PC}} = 2.4$ Hz, Ar- CH_3), 18.35 (s,

$\text{PCH}(\text{CH}_3)_2$), 17.76 (d, $^2J_{\text{PC}} = 1.5$ Hz, $\text{PCH}(\text{CH}_3)_2$). Assignment of the $^{13}\text{C}\{^1\text{H}\}$ NMR signals was confirmed by ^{13}C DEPT 135. Elemental analysis: Found: C, 58.35%; H, 8.88%. Calcd for $\text{C}_{19}\text{H}_{34}\text{P}_2\text{S}_2$: C, 58.73%; H, 8.82%.

Synthesis of Complex 2. To a solution of 90.5 mg (0.172 mmol) of $[\text{Rh}(\text{COE})_2(\text{acetone})_2]\text{BF}_4$ in 1.6 mL of acetone was added a solution of 67.2 mg (0.173 mmol) of ligand 1 in 1.9 mL of acetone, and the resulting solution was stirred at room temperature for 22 h, during which its color changed from orange to dark brown. The solution was then concentrated under vacuum to 1.1 mL and added to 17 mL of pentane, with stirring. The liquid phase was then decanted, and residual solvent was removed from the product under vacuum. The resulting solid was then crushed to powder and washed with 6 mL of pentane. Removal of residual solvent under vacuum yielded 98.9 mg (0.155 mmol, 90.4% yield) of the product as a dark brown powder. $^{31}\text{P}\{^1\text{H}\}$ NMR (202 MHz, acetone- d_6): 80.63 (bs). ^1H NMR (500 MHz, acetone- d_6): 7.56 (m, $^3J_{\text{HH}} = 7.7$ Hz, 2H, Ar-H), 7.22 (m, $^3J_{\text{HH}} = 7.7$ Hz, 1H, Ar-H), 2.84 (m, $^2J_{\text{PH}} = 13.9$ Hz, $^3J_{\text{HH}} = 6.9$ Hz, 2H, $\text{PCH}(\text{CH}_3)_2$), 2.67 (m, $^2J_{\text{PH}} = 14.2$ Hz, $^3J_{\text{HH}} = 7.1$ Hz, 2H, $\text{PCH}(\text{CH}_3)_2$), 1.37 (br s, 3H, Rh- CH_3), 1.31 (dd, $^3J_{\text{PH}} = 17.7$ Hz, $^3J_{\text{HH}} = 6.9$ Hz, 6H, $\text{PCH}(\text{CH}_3)_2$), 1.23 (dd, $^3J_{\text{PH}} = 17.9$ Hz, $^3J_{\text{HH}} = 6.9$ Hz, 6H, $\text{PCH}(\text{CH}_3)_2$), 1.17 (dd, $^3J_{\text{PH}} = 17.8$ Hz, $^3J_{\text{HH}} = 7.0$ Hz, 6H, $\text{PCH}(\text{CH}_3)_2$), 1.15 (dd, $^3J_{\text{PH}} = 17.6$ Hz, $^3J_{\text{HH}} = 7.0$ Hz, 6H, $\text{PCH}(\text{CH}_3)_2$). $^{13}\text{C}\{^1\text{H}\}$ NMR (126 MHz, acetone- d_6): 178.48 (bm, C_{ipso}), 145.78 (dd, $^1J_{\text{PC}} = 92.2$ Hz, $^3J_{\text{PC}} = 11.9$ Hz, Ar_{ortho}), 134.35 (m, Ar_{meta}), 121.07 (t, $^3J_{\text{PC}} = 11.8$ Hz, Ar_{para}), 29.96 (d, $^1J_{\text{PC}} = 44.7$ Hz, $\text{PCH}(\text{CH}_3)_2$), 27.59 (d, $^1J_{\text{PC}} = 43.8$ Hz, $\text{PCH}(\text{CH}_3)_2$), 17.24 (s, $\text{PCH}(\text{CH}_3)_2$), 16.99 (s, $\text{PCH}(\text{CH}_3)_2$), 16.28 (s, $\text{PCH}(\text{CH}_3)_2$), 15.77 (s, $\text{PCH}(\text{CH}_3)_2$), -6.77 (d, $^1J_{\text{RhC}} = 26.2$ Hz, Rh- CH_3). Assignment of the $^{13}\text{C}\{^1\text{H}\}$ NMR signals was confirmed by ^{13}C - ^1H heteronuclear correlation. $^{19}\text{F}\{^1\text{H}\}$ NMR (376 MHz, acetone- d_6): -152.51 (s, free BF_4). $^{31}\text{P}\{^1\text{H}\}$ NMR (202 MHz, CD_3OD): 79.00 (s). ^1H NMR (500 MHz, CD_3OD): 7.37 (m, $^3J_{\text{HH}} = 7.6$ Hz, 2H, Ar-H), 7.11 (m, $^3J_{\text{HH}} = 7.6$ Hz, 1H, Ar-H), 2.64 (m, $^3J_{\text{HH}} = 7.0$ Hz, 2H, $\text{PCH}(\text{CH}_3)_2$), 2.58 (m, $^3J_{\text{HH}} = 7.0$ Hz, 2H, $\text{PCH}(\text{CH}_3)_2$), 1.29 (dd, $^3J_{\text{PH}} = 17.6$ Hz, $^3J_{\text{HH}} = 6.9$ Hz, 12H, $\text{PCH}(\text{CH}_3)_2$), 1.18 (dd, $^3J_{\text{PH}} = 17.9$ Hz, $^3J_{\text{HH}} = 7.2$ Hz, 6H, $\text{PCH}(\text{CH}_3)_2$), 1.16 (d, $^2J_{\text{RhH}} = 2.1$ Hz, 3H, Rh- CH_3), 1.16 (dd, $^3J_{\text{PH}} = 17.8$ Hz, $^3J_{\text{HH}} = 7.1$ Hz, 6H, $\text{PCH}(\text{CH}_3)_2$). $^{13}\text{C}\{^1\text{H}\}$ NMR (126 MHz, CD_3OD): 180.75 (dt, $^1J_{\text{RhC}} = 39.9$ Hz, $^2J_{\text{PC}} = 17.9$ Hz, C_{ipso}), 145.36 (ddd, $^1J_{\text{PC}} = 93.2$ Hz, $^3J_{\text{PC}} = 12.3$ Hz, $J = 2.0$ Hz, Ar_{ortho}), 134.37 (m, Ar_{meta}), 120.76 (t, $^3J_{\text{PC}} = 11.9$ Hz, Ar_{para}), 29.85 (d, $^1J_{\text{PC}} = 44.7$ Hz, $\text{PCH}(\text{CH}_3)_2$), 29.34 (d, $^1J_{\text{PC}} = 43.5$ Hz, $\text{PCH}(\text{CH}_3)_2$), 17.52 (s, $\text{PCH}(\text{CH}_3)_2$), 17.34 (s, $\text{PCH}(\text{CH}_3)_2$), 16.33 (s, $\text{PCH}(\text{CH}_3)_2$), 16.07 (s, $\text{PCH}(\text{CH}_3)_2$), -8.78 (d, $^1J_{\text{RhC}} = 25.7$ Hz, Rh- CH_3). Assignment of the $^{13}\text{C}\{^1\text{H}\}$ NMR signals was confirmed by ^{13}C - ^1H heteronuclear correlation. $^{19}\text{F}\{^1\text{H}\}$ NMR (376 MHz, CD_3OD): -155.59 (s, free BF_4). $^{31}\text{P}\{^1\text{H}\}$ NMR (202 MHz, CD_3OD , -70 °C): 78.84 (s). ^1H NMR (500 MHz, CD_3OD , -70 °C): 7.43 (m, $^3J_{\text{HH}} = 7.7$ Hz, 2H, Ar-H), 7.12 (m, $^3J_{\text{HH}} = 7.7$ Hz, 1H, Ar-H), 2.65 (m, $^3J_{\text{HH}} = 7.0$ Hz, 4H, $\text{PCH}(\text{CH}_3)_2$), 1.30-1.12 (m, 24H, $\text{PCH}(\text{CH}_3)_2$), 1.04 (d, $^2J_{\text{RhH}} = 2.3$ Hz, 3H, Rh- CH_3). Selected $^{13}\text{C}\{^1\text{H}\}$ NMR (126 MHz, CD_3OD , -70 °C): 134.40 (m, Ar_{meta}), 120.69 (t, $^3J_{\text{PC}} = 11.8$ Hz, Ar_{para}), 29.77 (d, $^1J_{\text{PC}} = 44.8$ Hz, $\text{PCH}(\text{CH}_3)_2$), 28.46 (d, $^1J_{\text{PC}} = 44.5$ Hz, $\text{PCH}(\text{CH}_3)_2$), 17.34 (s, $\text{PCH}(\text{CH}_3)_2$), 17.13 (s, $\text{PCH}(\text{CH}_3)_2$), 16.22 (s, $\text{PCH}(\text{CH}_3)_2$), 15.64 (s, $\text{PCH}(\text{CH}_3)_2$), -8.38 (d, $^1J_{\text{RhC}} = 25.4$ Hz, Rh- CH_3). Assignment of the $^{13}\text{C}\{^1\text{H}\}$ NMR signals was confirmed by ^{13}C - ^1H heteronuclear correlation. $^{31}\text{P}\{^1\text{H}\}$ NMR (162 MHz, CD_3CN): 87.55 (s). ^1H NMR (400 MHz, CD_3CN): 7.34 (m, $^3J_{\text{HH}} = 7.7$ Hz, 2H, Ar-H), 7.13 (m, $^3J_{\text{HH}} = 7.7$ Hz, 1H, Ar-H), 2.58 (m, $^3J_{\text{HH}} = 7.0$ Hz, 2H, $\text{PCH}(\text{CH}_3)_2$), 2.51 (m, $^3J_{\text{HH}} = 7.0$ Hz, 2H, $\text{PCH}(\text{CH}_3)_2$), 1.23 (dd, $^3J_{\text{PH}} = 17.8$ Hz, $^3J_{\text{HH}} = 6.9$ Hz, 6H, $\text{PCH}(\text{CH}_3)_2$), 1.22 (dd, $^3J_{\text{PH}} = 17.7$ Hz, $^3J_{\text{HH}} = 6.9$ Hz, 6H, $\text{PCH}(\text{CH}_3)_2$), 1.13 (dd, $^3J_{\text{PH}} = 17.8$ Hz, $^3J_{\text{HH}} = 7.0$ Hz, 6H, $\text{PCH}(\text{CH}_3)_2$), 1.07 (dd, $^3J_{\text{PH}} = 17.9$ Hz, $^3J_{\text{HH}} = 7.0$ Hz, 6H, $\text{PCH}(\text{CH}_3)_2$), 0.90 (d, $^2J_{\text{RhH}} = 2.4$ Hz, 3H, Rh- CH_3). $^{13}\text{C}\{^1\text{H}\}$ NMR (101 MHz, CD_3CN): 184.47 (dt, $^1J_{\text{RhC}} = 35.5$ Hz, $^2J_{\text{PC}} = 20.8$ Hz, C_{ipso}), 142.44 (ddd, $^1J_{\text{PC}} = 92.2$ Hz, $^3J_{\text{PC}} = 13.5$ Hz, $J = 2.1$ Hz, Ar_{ortho}), 134.12 (m, Ar_{meta}), 121.15 (t, $^3J_{\text{PC}} = 11.7$ Hz, Ar_{para}), 30.21 (d, $^1J_{\text{PC}} = 44.3$ Hz, $\text{PCH}(\text{CH}_3)_2$), 28.04 (d, $^1J_{\text{PC}} = 43.7$ Hz, $\text{PCH}(\text{CH}_3)_2$), 17.25 (s, $\text{PCH}(\text{CH}_3)_2$), 17.02 (s, $\text{PCH}(\text{CH}_3)_2$), 16.18 (s, PCH

(CH₃)₂), 15.91 (s, PCH(CH₃)₂), -1.66 (d, ¹J_{RhC} = 21.9 Hz, Rh-CH₃). ¹⁹F{¹H} NMR (376 MHz, CD₃CN): -153.28 (s, free BF₄). Elemental analysis (acetone adduct): Found: C, 41.58%; H, 6.36%. Calcd for C₂₂H₄₀BF₄OP₂RhS₂: C, 41.52%; H, 6.34%.

X-ray Structural Analysis of Complex 2. Complex 2 was crystallized at -20 °C from an acetone solution overlaid with diethyl ether. CCDC deposition number: 745236. Crystal data: C₂₅H₄₆O₂P₂RhS₂ + BF₄, colorless needle, 0.12 × 0.10 × 0.08 mm³, monoclinic, P2₁/c, *a* = 8.8444(6) Å, *b* = 21.2018(14) Å, *c* = 17.7823(12) Å, β = 101.268(2)°, from 27° of data, *T* = 100(2) K, *V* = 3270.2(4) Å³, *Z* = 4, fw = 694.40 g mol⁻¹, *D*_c = 1.410 g cm⁻³, μ = 0.791 mm⁻¹. Data collection and processing: Bruker APEX-II KappaCCD diffractometer, Mo Kα (λ = 0.71073 Å), graphite monochromator, equipped with Miracol optics. 38418 reflections collected, -12 ≤ *h* ≤ 9, -30 ≤ *k* ≤ 26, -25 ≤ *l* ≤ 25, 2θ_{max} = 61.1°, (*R*-int = 0.0438). The data were processed with SAINT.²⁶ Solution and refinement: Structure was solved by direct methods with SHELXS and refined with SHELXL-97 using the full-matrix least-squares method based on *F*².²⁷ There are 350 parameters with no restraints, final *R*₁ = 0.0389 (based on *F*²) for data with *I* > 2σ(*I*) and *R*₁ = 0.0563 for 10 079 reflections, goodness of fit on *F*² = 1.070, largest electron density peak = 1.493 e Å⁻³.

In Situ Synthesis of Complex 2 in Acetone-*d*₆ and NMR Monitoring of the Reaction Progress. To a solution of 7.0 mg (0.013 mmol) of [Rh(COE)₂(acetone)₂]BF₄ in 0.2 mL of acetone-*d*₆ was added a solution of 5.2 mg (0.013 mmol) of ligand 1 in 0.5 mL of acetone-*d*₆. The resulting solution was stirred manually at room temperature for a few seconds and then loaded into an NMR tube. The sample was then placed in the NMR spectrometer, and ¹H NMR spectra were recorded at room temperature every 5 min. Gradual formation of complex 2 was observed, whereas no C–H cleavage products were detected. See above for NMR data of complex 2 in acetone-*d*₆.

In Situ Synthesis of Complex 2 in CD₃OD/CD₂Cl₂ and NMR Monitoring of the Reaction Progress. To a solution of 7.3 mg (0.014 mmol) of [Rh(COE)₂(acetone)₂]BF₄ in 0.3 mL of CD₃OD was added a solution of 5.4 mg (0.014 mmol) of ligand 1 in 0.3 mL of CD₂Cl₂. The resulting solution was stirred manually at room temperature for a few seconds and then loaded into an NMR tube. The sample was then placed in the NMR spectrometer, and ¹H NMR spectra were recorded at room temperature every 5 min. Gradual formation of complex 2 was observed, whereas no C–H cleavage products were detected. The following NMR data for complex 2 were collected after 1.5 h. ³¹P{¹H} NMR (162 MHz, CD₃OD:CD₂Cl₂): 78.94 (s). ¹H NMR (400 MHz, CD₃OD:CD₂Cl₂): 7.24 (m, ³J_{HH} = 7.7 Hz, 2H, Ar-*H*), 7.09 (m, ³J_{HH} = 7.7 Hz, 1H, Ar-*H*), 2.55 (m, ³J_{HH} = 7.0 Hz, 2H, PCH(CH₃)₂), 2.48 (m, ³J_{HH} = 7.0 Hz, 2H, PCH(CH₃)₂), 1.31–1.24 (m, 12H, PCH(CH₃)₂), 1.21 (s, 3H, Rh-CH₃; overlaps with isopropyl signals), 1.17 (dd, ³J_{PH} = 17.8 Hz, ³J_{HH} = 7.1 Hz, 6H, PCH(CH₃)₂), 1.17 (dd, ³J_{PH} = 17.6 Hz, ³J_{HH} = 7.1 Hz, 12H, PCH(CH₃)₂). Assignment of the ¹H NMR signals was confirmed by ¹³C–¹H heteronuclear correlation. Selected ¹³C{¹H} NMR (126 MHz, CD₃OD:CD₂Cl₂): -8.74 (d, ¹J_{RhC} = 26.0 Hz, Rh-CH₃).

In Situ Synthesis of Complex 2 in THF-*d*₈/CD₂Cl₂ and NMR Monitoring of the Reaction Progress. To a suspension of 10.5 mg (0.015 mmol) of [Rh(COE)₂Cl]₂ in 0.45 mL of THF was added a solution of 5.7 mg (0.029 mmol) of AgBF₄ in 0.45 mL of THF, and the resulting mixture was stirred in the dark, at room temperature, for 30 min. This mixture was then filtered via a cotton pad to afford a clear orange solution. The solvent was then removed under vacuum, and the resulting residue was dissolved in 0.3 mL of THF-*d*₈. To this solution was then added a solution of 11.3 mg (0.029 mmol) of ligand 1 in 0.3 mL of CD₂Cl₂, and the resulting solution was stirred manually at room temperature for a few seconds and then loaded into an NMR tube. The sample was then placed in the NMR spectrometer, and ¹H NMR spectra were recorded at room temperature every 5 min. Gradual formation of complex 2 was observed, whereas no C–H cleavage products were detected. The following NMR data for complex 2 were collected after 3.5 h. ³¹P{¹H} NMR (162 MHz, THF-*d*₈:CD₂Cl₂): 77.45 (bs). ¹H NMR (400 MHz, THF-*d*₈:CD₂Cl₂): 7.35 (m, ³J_{HH} =

7.6 Hz, 2H, Ar-*H*), 7.13 (m, ³J_{HH} = 7.6 Hz, 1H, Ar-*H*), 2.64 (m, ²J_{PH} = ³J_{HH} = 6.9 Hz, 2H, PCH(CH₃)₂), 2.46 (m, ²J_{PH} = ³J_{HH} = 7.0 Hz, 2H, PCH(CH₃)₂), 1.31 (br s, 3H, Rh-CH₃; overlaps with isopropyl signals), 1.23 (dd, ³J_{PH} = 17.7 Hz, ³J_{HH} = 6.9 Hz, 12H, PCH(CH₃)₂), 1.13 (dd, ³J_{PH} = 18.0 Hz, ³J_{HH} = 7.1 Hz, 6H, PCH(CH₃)₂), 1.10 (dd, ³J_{PH} = 17.7 Hz, ³J_{HH} = 7.0 Hz, 6H, PCH(CH₃)₂). Assignment of the ¹H NMR signals was confirmed by ¹³C–¹H heteronuclear correlation. Selected ¹³C{¹H} NMR (126 MHz, THF-*d*₈:CD₂Cl₂): -9.74 (bm, Rh-CH₃).

In Situ Synthesis of Complex 2 in CD₃CN/Acetone-*d*₆ and NMR Monitoring of the Reaction Progress. To a solution of 5.8 mg (0.015 mmol) of ligand 1 in 0.3 mL of acetone-*d*₆ was added 12 mg (0.272 mmol) of CD₃CN. The resulting solution was then mixed at room temperature with a solution containing 7.9 mg (0.015 mmol) of [Rh(COE)₂(acetone)₂]BF₄ in 0.5 mL of acetone-*d*₆. The afforded solution was then loaded into an NMR tube and placed in an NMR spectrometer that was preheated to 60 °C. ¹H NMR spectra of the solution were then recorded at 60 °C every 10–15 min. Gradual formation of complex 2 was observed, whereas no C–H cleavage products were detected. The following NMR data for complex 2 were collected after 1 h. ³¹P{¹H} NMR (202 MHz, CD₃CN:acetone-*d*₆, 60 °C): 87.42 (s). ¹H NMR (500 MHz, CD₃CN:acetone-*d*₆, 60 °C): 7.52 (m, ³J_{HH} = 7.7 Hz, 2H, Ar-*H*), 7.20 (m, ³J_{HH} = 7.7 Hz, 1H, Ar-*H*), 2.74 (m, ³J_{HH} = 7.0 Hz, 2H, PCH(CH₃)₂), 2.64 (m, ³J_{HH} = 7.0 Hz, 2H, PCH(CH₃)₂), 1.31 (dd, ³J_{PH} = 13.3 Hz, ³J_{HH} = 7.3 Hz, 6H, PCH(CH₃)₂), 1.28 (dd, ³J_{PH} = 13.5 Hz, ³J_{HH} = 7.2 Hz, 12H, PCH(CH₃)₂), 1.19 (dd, ³J_{PH} = 11.1 Hz, ³J_{HH} = 7.2 Hz, 6H, PCH(CH₃)₂), 1.15 (dd, ³J_{PH} = 11.1 Hz, ³J_{HH} = 7.2 Hz, 12H, PCH(CH₃)₂), 1.11 (d, ²J_{RhH} = 2.4 Hz, 3H, Rh-CH₃).

Computational Methods. All calculations were carried out using the Gaussian 03 software package.²⁸ Geometry optimizations and evaluation of harmonic frequencies were performed at the DFT level,²⁹ using the PBE0³⁰ hybrid density functional in conjunction with the PC-1 basis set. The latter consists of the SDD basis set³¹ with an added *f* function for rhodium (exponent 1.062, the geometric mean of the 2*f* exponents given by Martin and Sundermann³²), together with Jensen's "polarization consistent" pc-1 basis set for the remaining elements.³³ This combination is of double-ζ plus polarization quality. The model structures used for the calculations featured CH₃ groups instead of the *i*Pr substituents on the phosphorus atoms. Test calculations using the full experimental structures afforded results that are qualitatively similar to the model systems. The accuracy of the computational method in predicting the geometries of complexes was validated by calculating the geometry of complex 2, for which the crystal structure is known. All structures were fully optimized in the gas phase and characterized as minima or transition states by calculating the harmonic vibrational frequencies. The reaction pathways for C–C and C–H cleavage were traced from the corresponding transition states to the products and to the reactants using the intrinsic reaction coordinate (IRC) method.³⁴ The energetic data are presented as free energies (Δ*G*) at 298.15 K and include corrections for solvation and dispersion (see below).

Bulk solvent effects of the experimental acetone and methanol media have been taken into account via the self-consistent reaction field (SCRf) method, using the continuum solvation model COSMO (conductor-like screening model) as it is implemented in Gaussian 03.³⁵ In this model, the solvent is represented by an infinite dielectric medium characterized by the relative dielectric constant of the bulk solvent (ε = 20.7 for acetone), and the effective cavity occupied by the solute in the solvent is calculated on the basis of the united atom (UA0) topological model radii. Gas-phase optimized geometries were used in single-point calculations at the COSMO level.

Dispersion interactions within the computed structures were also taken into account. These weak interactions are usually poorly described by DFT methods, but can amount to 10–20 kcal mol⁻¹ for dissociation and atomization energies of large systems.³⁶ In the present work, these interactions were included by adding an empirical dispersion correction term, as was proposed by Grimme and co-workers,^{36a–c} with a value of *s*₆ = 0.7. This value was suggested by Karton et al. for the PBE0 functional.^{36d} For the problem at hand, the

largest effect of the dispersion correction was to increase the interaction energy between 4' and *cis*-2-butene with formation of 5' from 20.1 to 26.0 kcal mol⁻¹.

Charge decomposition analysis (CDA)^{37,38} was applied for the quantification of electron transfers at critical points along the potential energy surfaces of the SCS system.

■ ASSOCIATED CONTENT

Supporting Information

Crystallographic data (CIF) and optimized geometries for computed structures (*xyz* coordinates). This material is available free of charge via the Internet at <http://pubs.acs.org>.

■ AUTHOR INFORMATION

Corresponding Author

*E-mail: david.milstein@weizmann.ac.il.

Present Address

[§]Department of Chemistry, University of North Texas, Denton, TX 76203, USA.

Author Contributions

^{||}These authors contributed equally.

■ ACKNOWLEDGMENTS

This research was supported by the European Research Council under the FP7 framework (ERC No 246837); by the Israel Science Foundation; by the MINERVA Foundation; and by the Kimmel Center for Molecular design. D.M. holds the Israel Matz Professorial Chair of Organic Chemistry. I.E. gratefully acknowledges financial support from the Ministry of Immigrant Absorption, State of Israel.

■ REFERENCES

(1) General reviews on C–C activation: (a) Rybtchinski, B.; Milstein, D. *Angew. Chem., Int. Ed.* **1999**, *38*, 870–883. (b) Murakami, M.; Ito, Y. In *Topics in Organometallic Chemistry*; Murai, S., Ed.; Springer-Verlag: New York, 1999; Vol. 3, pp 97–129. (c) Jun, C.-H.; Monn, C. W.; Lee, D.-Y. *Chem.—Eur. J.* **2002**, *8*, 2422–2428. (d) Jun, C.-H. *Chem. Soc. Rev.* **2004**, *33*, 610–618.

(2) For a selection of recently reported activations of nonstrained C–C single bonds, see: (a) Zhang, X.; Emge, T. J.; Ghosh, R.; Goldman, A. S. *J. Am. Chem. Soc.* **2005**, *127*, 8250–8251. (b) Celenligil-Cetin, R.; Watson, L. A.; Guo, C.; Foxman, B. M.; Ozerov, O. V. *Organometallics* **2005**, *24*, 186–189. (c) Dewhurst, R. D.; Hill, A. F.; Rae, A. D.; Willis, A. C. *Organometallics* **2005**, *24*, 4703–4706. (d) Li, X.; Sun, H.; Yu, F.; Floerke, U.; Klein, H.-F. *Organometallics* **2006**, *25*, 4695–4697. (e) Ochiai, M.; Hashimoto, H.; Tobita, H. *Angew. Chem., Int. Ed.* **2007**, *46*, 8192–8194. (f) Baker, M. V.; Brown, D. H.; Hesler, V. J.; Skelton, B. W.; White, A. H. *Organometallics* **2007**, *26*, 250–252. (g) Baksi, S.; Acharyya, R.; Basuli, F.; Peng, S.-M.; Lee, G.-H.; Nethaji, M.; Bhattacharya, S. *Organometallics* **2007**, *26*, 6596–6603. (h) Chan, K. S.; Li, X. Z.; Dzik, W. I.; de Bruin, B. *J. Am. Chem. Soc.* **2008**, *130*, 2051–2061. (i) Atesin, T. A.; Li, T.; Lachaize, S.; Garcia, J. J.; Jones, W. D. *Organometallics* **2008**, *27*, 3811–3817. (j) Zhao, P.; Hartwig, J. F. *Organometallics* **2008**, *27*, 4749–4757. (k) Gunay, A.; Muller, C.; Lachicotte, R. J.; Brennessel, W. W.; Jones, W. D. *Organometallics* **2009**, *28*, 6524–6530. (l) Lai, T. H.; Chan, K. S. *Organometallics* **2009**, *28*, 6845–6846. (m) Bolano, T.; Buil, M. L.; Esteruelas, M. A.; Izquierdo, S.; Lalrempuia, R.; Oliván, M.; Onate, E. *Organometallics* **2010**, *29*, 4517–4523. (n) Chan, Y. W.; Chan, K. S. *J. Am. Chem. Soc.* **2010**, *132*, 6920–6922. (o) Grochowski, M. R.; Li, T.; Brennessel, W. W.; Jones, W. D. *J. Am. Chem. Soc.* **2010**, *132*, 12412–12421. (p) Evans, M. E.; Li, T.; Jones, W. D. *J. Am. Chem. Soc.* **2010**, *132*, 16278–16284. (q) Obenhuber, A.; Ruhland, K. *Organometallics* **2011**, *30*, 171–186. (r) Swartz, B. D.; Brennessel, W. W.; Jones, W. D. *Organometallics* **2011**, *30*, 1523–1529. (s) Lee, S. Y.; Lai, T. H.; Choi, K. S.; Chan, K. S. *Organometallics* **2011**, *30*, 3691–3693.

(3) Reviews on C–C activation in pincer systems: (a) van der Boom, M. E.; Milstein, D. *Chem. Rev.* **2003**, *103*, 1759–1792. (b) Milstein, D. *Pure Appl. Chem.* **2003**, *75*, 445–460. (c) Rybtchinski, B.; Milstein, D. *ACS Symp. Ser.* **2004**, *885*, 70–85. (d) Rybtchinski, B.; Milstein, D. In *The Chemistry of Pincer Compounds*; Morales-Morales, D., Jensen, C. M., Eds.; Elsevier: Amsterdam, 2007; pp 87–105. (e) Albrecht, M.; Lindner, M. M. *Dalton Trans.* **2011**, *40*, 8733–8744.

(4) C–C bond cleavage has been studied extensively in our group using pincer ligands with phosphorus donor groups. For further details, see: (a) Gozin, M.; Weisman, A.; Ben-David, Y.; Milstein, D. *Nature* **1993**, *364*, 699–701. (b) Gozin, M.; Aizenberg, M.; Liou, S.-Y.; Weisman, A.; Ben-David, Y.; Milstein, D. *Nature* **1994**, *370*, 42–44. (c) Liou, S.-Y.; Gozin, M.; Milstein, D. *J. Am. Chem. Soc.* **1995**, *117*, 9774–9775. (d) Rybtchinski, B.; Vignalok, A.; Ben-David, Y.; Milstein, D. *J. Am. Chem. Soc.* **1996**, *118*, 12406–12415. (e) Gandelman, M.; Vignalok, A.; Shimon, L. J. W.; Milstein, D. *Organometallics* **1997**, *16*, 3981–3986. (f) Liou, S.-Y.; van der Boom, M. E.; Milstein, D. *Chem. Commun.* **1998**, *6*, 687–688. (g) van der Boom, M. E.; Ben-David, Y.; Milstein, D. *Chem. Commun.* **1998**, *8*, 917–918. (h) van der Boom, M. E.; Liou, S.-Y.; Ben-David, Y.; Gozin, M.; Milstein, D. *J. Am. Chem. Soc.* **1998**, *120*, 13415–13421. (i) Rybtchinski, B.; Milstein, D. *J. Am. Chem. Soc.* **1999**, *121*, 4528–4529. (j) van der Boom, M. E.; Ben-David, Y.; Milstein, D. *J. Am. Chem. Soc.* **1999**, *121*, 6652–6656. (k) van der Boom, M. E.; Kraatz, H.-B.; Hassner, L.; Ben-David, Y.; Milstein, D. *Organometallics* **1999**, *18*, 3873–3884. (l) Cohen, R.; van der Boom, M. E.; Shimon, L. J. W.; Rozenberg, H.; Milstein, D. *J. Am. Chem. Soc.* **2000**, *122*, 7723–7734. (m) Gandelman, M.; Vignalok, A.; Konstantinovskii, L.; Milstein, D. *J. Am. Chem. Soc.* **2000**, *122*, 9848–9849. (n) Rybtchinski, B.; Oevers, S.; Montag, M.; Vignalok, A.; Rozenberg, H.; Martin, J. M. L.; Milstein, D. *J. Am. Chem. Soc.* **2001**, *123*, 9064–9077. (o) Gauvin, R. M.; Rozenberg, H.; Shimon, L. J. W.; Milstein, D. *Organometallics* **2001**, *20*, 1719–1724. (p) Gandelman, M.; Shimon, L. J. W.; Milstein, D. *Chem.—Eur. J.* **2003**, *9*, 4295–4300. (q) van der Boom, M. E.; Liou, S.-Y.; Shimon, L. J. W.; Ben-David, Y.; Milstein, D. *Inorg. Chim. Acta* **2004**, *357*, 4015–4023. (r) Salem, H.; Ben-David, Y.; Shimon, L. J. W.; Milstein, D. *Organometallics* **2006**, *25*, 2292–2300. (s) Gauvin, R. M.; Rozenberg, H.; Shimon, L. J. W.; Ben-David, Y.; Milstein, D. *Chem.—Eur. J.* **2007**, *13*, 1382–1393. (t) Frech, C. M.; Shimon, L. J. W.; Milstein, D. *Chem.—Eur. J.* **2007**, *13*, 7501–7509.

(5) Reactions involving C–C bond cleavage in amine-based, NCN-type complexes have been studied by van Koten and co-workers. See: (a) Grove, D. M.; van Koten, G.; Ubbels, H. J. C. *Organometallics* **1982**, *1*, 1366–1370. (b) Albrecht, M.; Gossage, R. A.; Spek, A. L.; van Koten, G. *J. Am. Chem. Soc.* **1999**, *121*, 11898–11899. (c) Albrecht, M.; Spek, A. L.; van Koten, G. *J. Am. Chem. Soc.* **2001**, *123*, 7233–7246.

(6) (a) Mézailles, N.; Le Floch, P. In *The Chemistry of Pincer Compounds*; Morales-Morales, D., Jensen, C. M., Eds.; Elsevier: Amsterdam, 2007; pp 235–271. (b) Odinet, I. L.; Aleksanyan, D. V.; Kozlov, V. A. *Lett. Org. Chem.* **2010**, *7*, 583–595.

(7) The new ligand **1** was prepared in analogy to a literature procedure. See: Kanbara, T.; Yamamoto, T. *J. Organomet. Chem.* **2003**, *688*, 15–19. Details regarding the present synthetic methodology are given in the Experimental Section.

(8) About 65% conversion was observed within 1 h at room temperature for initial concentrations $[1]_0 = [[\text{Rh}(\text{COE})_2(\text{acetone})_2]\text{BF}_4]_0 \approx 20$ mM. The degree of conversion was estimated on the basis of ¹H NMR signal integration, using the arene hydrogen signals.

(9) A complex of rhodium with an adventitious ketol ligand has been previously reported by our group. See: Rybtchinski, B.; Konstantinovskii, L.; Shimon, L. J. W.; Vignalok, A.; Milstein, D. *Chem.—Eur. J.* **2000**, *6*, 3287–3292.

(10) Complex **2** is sparingly soluble in neat THF, precluding NMR monitoring of the reaction in this solvent, and therefore, dichloromethane was added to increase solubility. The reaction was carried out at room temperature and monitored periodically by ¹H NMR spectroscopy.

(11) Ligand **1** is sparingly soluble in neat methanol, and therefore, dichloromethane was added to increase solubility. The reaction was carried out at room temperature and monitored periodically by ^1H NMR spectroscopy.

(12) No reaction was observed when acetonitrile was used as a neat solvent, and it was, therefore, added in a smaller amount to an acetone solution containing $[\text{Rh}(\text{COE})_2(\text{acetone})_2]\text{BF}_4$ and **1**. Even under these conditions, the reaction was prohibitively slow at room temperature, and the solution was, therefore, heated at 60°C and monitored periodically by ^1H NMR spectroscopy. At this temperature, 20% conversion was obtained within 1 h (for initial concentrations $[\mathbf{1}]_0 = [[\text{Rh}(\text{COE})_2(\text{acetone})_2]\text{BF}_4]_0 \approx 20\text{ mM}$).

(13) Gandelman, M.; Vignalok, A.; Shimon, L. J. W.; Milstein, D. *Organometallics* **1997**, *16*, 3981–3986.

(14) Salem, H.; Ben-David, Y.; Shimon, L. J. W.; Milstein, D. *Organometallics* **2006**, *25*, 2292–2300.

(15) The $\text{C}_{\text{Ar}}\text{--P}$ and $\text{P}\text{--S}$ bonds of the SCS ligand in complex **2** measure 1.8 and 2.0 Å, respectively. By contrast, the $\text{C}_{\text{Ar}}\text{--C}$ and $\text{C}\text{--P}$ bonds of analogous PCP complexes measure around 1.5 and 1.8 Å, respectively.

(16) (a) Sundermann, A.; Uzan, O.; Milstein, D.; Martin, J. M. L. *J. Am. Chem. Soc.* **2000**, *122*, 7095–7104. (b) Cao, Z.; Hall, M. B. *Organometallics* **2000**, *19*, 3338–3346. (c) Sundermann, A.; Uzan, O.; Martin, J. M. L. *Organometallics* **2001**, *20*, 1783–1791. (d) Cohen, R.; Milstein, D.; Martin, J. M. L. *Organometallics* **2004**, *23*, 2336–2342.

(17) For the ancillary ligands CH_2O and BF_4^- , both complexes **4'** and **5'** were located as individual minima on the PES. However, a transition state for the $4' \rightarrow 5'$ transformation could not be found, since its barrier is very flat and is, therefore, masked by the transition states for $\text{C}\text{--H}$ and $\text{C}\text{--C}$ cleavage, both of which have very close geometries (see below).

(18) For recent reviews of $\text{C}\text{--H}$ agostic interactions, see: (a) Brookhart, M.; Green, M. L. H.; Parkin, G. *Proc. Natl. Acad. Sci. U.S.A.* **2007**, *104*, 6908–6914. (b) Lein, M. *Coord. Chem. Rev.* **2009**, *253*, 625–634. (c) Balcells, D.; Clot, E.; Eisenstein, O. *Chem. Rev.* **2010**, *110*, 749–823. (d) Omae, I. *J. Organomet. Chem.* **2011**, *696*, 1128–1145.

(19) (a) Tomaszewski, R.; Hyla-Kryspin, I.; Mayne, C. L.; Arif, A. M.; Gleiter, R.; Ernst, R. D. *J. Am. Chem. Soc.* **1998**, *120*, 2959–2960. (b) Vignalok, A.; Rybtchinski, B.; Shimon, L. J. W.; Ben-David, Y.; Milstein, D. *Organometallics* **1999**, *18*, 895–905. (c) Jaffart, J.; Cole, M. L.; Etienne, M.; Reinhold, M.; McGrady, J. E.; Maseras, F. *Dalton Trans.* **2003**, 4057–4064. (d) Harvey, B. G.; Mayne, C. L.; Arif, A. M.; Ernst, R. D. *J. Am. Chem. Soc.* **2005**, *127*, 16426–16435. (e) Summerscales, O. T.; Cloke, F. G. N.; Hitchcock, P. B.; Green, J. C.; Hazari, N. *Science* **2006**, *311*, 829–831. (f) Harvey, B. G.; Arif, A. M.; Ernst, R. D. *J. Organomet. Chem.* **2006**, *691*, S211–S217. (g) Madison, B. L.; Thyme, S. B.; Keene, S.; Williams, B. S. *J. Am. Chem. Soc.* **2007**, *129*, 9538–9539. (h) Brayshaw, S. K.; Scats, E. L.; Green, J. C.; Weller, A. S. *Proc. Natl. Acad. Sci. U.S.A.* **2007**, *104*, 6921–6926. (i) Boulho, C.; Keys, T.; Coppel, Y.; Vendier, L.; Etienne, M.; Locati, A.; Bessac, F.; Maseras, F.; Pantazis, D. A.; McGrady, J. E. *Organometallics* **2009**, *28*, 940–943. (j) Scheins, S.; Messerschmidt, M.; Gembicky, M.; Pitak, M.; Volkov, A.; Coppens, P.; Harvey, B. G.; Turpin, G. C.; Arif, A. M.; Ernst, R. D. *J. Am. Chem. Soc.* **2009**, *131*, 6154–6160. (k) Chaplin, A. B.; Green, J. C.; Weller, A. S. *J. Am. Chem. Soc.* **2011**, *133*, 13162–13168.

(20) Scherer, W.; Herz, V.; Brück, A.; Hauf, C.; Reiner, F.; Altmannshofer, S.; Leusser, D.; Stalke, D. *Angew. Chem., Int. Ed.* **2011**, *50*, 2845–2849.

(21) Mayer, L.; Bakó, I.; Stirling, A. *J. Phys. Chem. A* **2011**, *115*, 12733–12737.

(22) The energy of interaction between the fragments of the complex was calculated within the CDA scheme for their geometries and interfragment distances adopted in the complex. The calculation does not involve the relaxation energy of the fragments caused by coordination.

(23) It should be noted that, in the experimental system, complex **2** is not observed as the adduct of COE, but rather of acetone. Unlike **5'**,

the stability of the olefin adduct of **2'** is comparable to that of its BF_4^- and CH_2O adducts. Because, in the experimental system, the concentration of the solvent acetone is much higher than that of the olefin, the latter is easily displaced by the solvent, leading to the acetone adduct.

(24) Windmüller, B.; Nürnberg, O.; Wolf, J.; Werner, H. *Eur. J. Inorg. Chem.* **1999**, 613–619 The procedure was modified by using AgBF_4 instead of AgPF_6 and conducting the whole process at room temperature.

(25) Farrugia, L. J. *J. Appl. Crystallogr.* **1997**, *30*, 565.

(26) BRUKER APEX-II software program package.

(27) Sheldrick, G. M. *Acta Crystallogr., Sect. A* **2008**, *64*, 112–122.

(28) Frisch, M. J.; Trucks, G. W.; Schlegel, H. B.; Scuseria, G. E.; Robb, M. A.; Cheeseman, J. R.; Montgomery, Jr., J. A.; Vreven, T.; Kudin, K. N.; Burant, J. C.; Millam, J. M.; Iyengar, S. S.; Tomasi, J.; Barone, V.; Mennucci, B.; Cossi, M.; Scalmani, G.; Rega, N.; Petersson, G. A.; Nakatsuji, H.; Hada, M.; Ehara, M.; Toyota, K.; Fukuda, R.; Hasegawa, J.; Ishida, M.; Nakajima, T.; Honda, Y.; Kitao, O.; Nakai, H.; Klene, M.; Li, X.; Knox, J. E.; Hratchian, H. P.; Cross, J. B.; Bakken, V.; Adamo, C.; Jaramillo, J.; Gomperts, R.; Stratmann, R. E.; Yazyev, O.; Austin, A. J.; Cammi, R.; Pomelli, C.; Ochterski, J. W.; Ayala, P. Y.; Morokuma, K.; Voth, G. A.; Salvador, P.; Dannenberg, J. J.; Zakrzewski, V. G.; Dapprich, S.; Daniels, A. D.; Strain, M. C.; Farkas, O.; Malick, D. K.; Rabuck, A. D.; Raghavachari, K.; Foresman, J. B.; Ortiz, J. V.; Cui, Q.; Baboul, A. G.; Clifford, S.; Cioslowski, J.; Stefanov, B. B.; Liu, G.; Liashenko, A.; Piskorz, P.; Komaromi, I.; Martin, R. L.; Fox, D. J.; Keith, T.; Al-Laham, M. A.; Peng, C. Y.; Nanayakkara, A.; Challacombe, M.; Gill, P. M. W.; Johnson, B.; Chen, W.; Wong, M. W.; Gonzalez, C.; Pople, J. A. *Gaussian 03*, revision E.01; Gaussian, Inc.: Wallingford, CT, 2004.

(29) (a) Kohn, W.; Sham, L. J. *Phys. Rev.* **1965**, *140*, A1133–A1138. (b) Parr, R. G.; Yang, W. *Density Functional Theory of Atoms and Molecules*; Oxford University Press: New York, 1970; p 230.

(30) Adamo, C.; Cossi, M.; Barone, V. *J. Mol. Struct. (THEOCHEM)* **1999**, *493*, 145–157.

(31) Dolg, M. In *Modern Methods and Algorithms of Quantum Chemistry*; Grotendorst, J., Ed.; Forschungszentrum Jülich: Jülich, Germany, 2000; Vol. 1, pp 479–508.

(32) Martin, J. M. L.; Sundermann, A. *J. Chem. Phys.* **2001**, *114*, 3408–3420.

(33) Jensen, F. *J. Chem. Phys.* **2002**, *116*, 7372–7379.

(34) (a) Gonzalez, C.; Schlegel, H. B. *J. Chem. Phys.* **1989**, *90*, 2154–2161. (b) Gonzalez, C.; Schlegel, H. B. *J. Phys. Chem.* **1990**, *94*, 5523–5527.

(35) (a) Klamt, A.; Schüürmann, G. *J. Chem. Soc., Perkin Trans. 2* **1993**, 799–805. (b) Barone, V.; Cossi, M. *J. Phys. Chem. A* **1998**, *112*, 1995–2001.

(36) (a) Grimme, S. *J. Comput. Chem.* **2006**, *27*, 1787–1799. (b) Schwabe, T.; Grimme, S. *Phys. Chem. Chem. Phys.* **2007**, *9*, 3397–3406. (c) Schwabe, T.; Grimme, S. *Acc. Chem. Res.* **2008**, *41*, 569–579.

(d) Karton, A.; Tarnopolsky, A.; Lamère, J.-F.; Schatz, G. C.; Martin, J. M. L. *J. Phys. Chem. A* **2008**, *112*, 12868–12886. (e) Karton, A.; Gruzman, D.; Martin, J. M. L. *J. Phys. Chem. A* **2009**, *113*, 8434–8447.

(37) Dapprich, S.; Frenking, G. *J. Phys. Chem.* **1995**, *99*, 9352–9362.

(38) The program CDA2.1 was used. It is available from <http://www.uni-marburg.de/fb15/ag-frenking/cda>.